Relocation effect and polarization mixing of surface acoustic waves in AlN-GaN bilayers on Al_2O_3(0001) substrates

Y. Takagaki
Paul-Drude-Institut für Festkörperelektronik, Hausvogteiplatz 5-7, 10117 Berlin, Germany

E. Chilla
Vectron International, Tele Filter, Potsdamer Str. 18, 14513 Teltow, Germany

(Received 20 February 2007; accepted 13 April 2007; published online 13 June 2007)

On the surface capped by an AlN-GaN bilayer, the particle displacements of surface acoustic waves (SAWs) are localized in the short-wavelength regime in the buried GaN layer instead of the overlaying AlN layer as a consequence of the significantly faster propagation of sound in AlN than in GaN. We numerically explore this relocation effect for Al_2O_3(0001) substrates, which are the commonly used substrate for group-III nitrides. We show that the critical wavelength for the relocation effect can be manipulated in a wide range by varying the thickness of the AlN layer owing to the moderate sound velocity in Al_2O_3. We also investigate the influences of the polarization mixing on the dispersion of SAWs. The SAW dispersion in the layered system is interpreted in terms of the anticrossing of relevant acoustic modes. © *2007 American Institute of Physics*.
[DOI: 10.1063/1.2740358]

The stiffness and durability of AlN make it one of the useful materials for high-frequency surface-acoustic-wave (SAW) devices.[1–5] The large piezoelectric coupling[6–8] in AlN and GaN is promising also in developing new functionalities based on the modulation of the optical and electrical properties of GaN by the SAW-induced piezoelectric fields. In designing such functional devices, a beneficial phenomenon was predicted numerically.[9,10] That is, the particle displacements of SAWs in a layered system containing a GaN layer covered by an (Al,Ga)N layer are enlarged in the GaN layer. The effect originates from the expulsion of acoustic waves from the fast-velocity (Al,Ga)N layer to the slow-velocity GaN layer. Due to the large velocity mismatch between AlN and GaN, the amplitude enhancement can be significant to the extent that even the fundamental SAW mode is almost completely localized in the buried layer. The resultant concentration of the SAW-induced piezoelectric fields in the GaN layer, which is typically the active layer in existing devices, is attractive for achieving high modulation efficiencies using SAWs. We point out that the sound velocity of a material having a large bandgap is generally large and, therefore, the SAW confinement effect can be exploited in a variety of material systems.

The relocation of SAWs from the top layer to a buried layer was initially predicted for an epitaxial AlN/GaN/$LiAlO_3$ system,[9] in which the GaN layer is oriented to exhibit the nonpolar M-plane surface. As $LiAlO_3$, whose crystal structure is tetragonal, is rather an unconventional substrate, the phenomenon was later examined for an AlN/GaN/SiC system.[10] The latter system was chosen as it possesses homogeneous hexagonal crystal structure and C-plane surface orientation. The relocation effect can, therefore, be confirmed to originate from the mismatch in the sound velocity but not in the crystal properties. However, as the sound velocity in SiC is even larger than that in AlN, the SAWs were found to be repelled strongly from the substrate, thereby considerably diminishing the relocation effect. The latter investigation revealed, in addition, peculiar mode slips in the dispersion of higher-lying SAW modes.[10]

Material substrates which are capable of supporting high-velocity acoustic propagation have attracted attention for the purpose of device application. Most popular high-velocity substrates, e.g., diamond, SiC, and Si, are, however, nonpiezoelectric, hindering them from effective incorporation in acoustically driven signal processing. Piezoelectric capping layers deposited on top of the high-velocity substrates allow for direct electrical excitation of acousto-elastic modes. For this reason, layered systems have been investigated intensively for some time. Interestingly, these systems also exhibit a variety of wave propagation phenomena that do not exist in bulk substrates, examples of which we mentioned above. Additionally, crystalline anisotropy and electro-acoustic coupling due to piezoelectricity increase the complexity of the system significantly.

In this paper, we examine the SAW relocation effect in an AlN/GaN/Al_2O_3(0001) system. Al_2O_3 is the most common substrate employed for the epitaxial growth of group-III nitrides. A comparison of the numerical results for the three cases of different substrates enables us to identify the origin of distinct features in the SAW dispersion. We show that, owing to the moderate SAW velocity in Al_2O_3, the relocation effect can be tailored to a large extent by varying the layer thicknesses. A prominent characteristic of the present system from the viewpoint of the acoustic propagation is that the trigonal crystal structure of Al_2O_3 mixes the sagittal and transversal polarizations of SAWs, except for specific propagation directions.[11] We interpret the SAW dispersion in terms of the anticrossing of various acoustic modes and reveal the role of the polarization mixture. The anticrossing explains also the peculiar feature of higher-lying SAW modes observed for the AlN/GaN/SiC system.

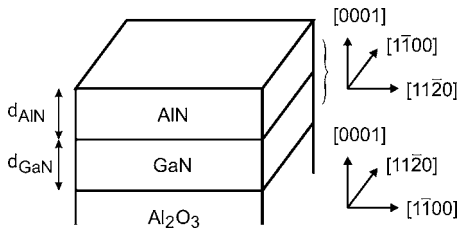

FIG. 1. Schematic of layered system. A (0001)-oriented hexagonal AlN/GaN bilayer is placed on a trigonal Al_2O_3(0001) substrate. The crystal orientation relationship is indicated on the right-hand side. The thickness of the AlN and GaN layers is d_{AlN} and d_{GaN}, respectively.

In order to clarify the essential characteristics of the SAW relocation effect when the substrate is Al_2O_3, we consider the simplest system illustrated in Fig. 1. We investigate the SAW propagation in (0001)-oriented AlN and GaN layers stacked on a Al_2O_3(0001) substrate. The thicknesses of the GaN and AlN layers are d_{GaN} and d_{AlN}, respectively. Although the elastic properties in the C-plane of hexagonal crystals are isotropic, the SAW properties in this layered system are no longer isotropic due to the trigonal crystal structure of Al_2O_3. We assume the usual crystal orientation relationship between the AlN/GaN bilayer and the Al_2O_3 substrate: The [1$\bar{1}$00] and [11$\bar{2}$0] directions in one component is parallel to the [11$\bar{2}$0] and [1$\bar{1}$00] directions in the other, respectively.

We evaluate the SAW dispersion by numerically solving the coupled equations

$$c_{ijkl}\frac{\partial^2 u_k}{\partial x_l\,\partial x_i} - \rho\frac{\partial^2 u_j}{\partial t^2} + e_{kij}\frac{\partial^2 \Phi}{\partial x_k\,\partial x_i} = 0, \tag{1}$$

$$e_{ijk}\frac{\partial^2 u_j}{\partial x_k\,\partial x_i} - \varepsilon_{ij}\frac{\partial^2 \Phi}{\partial x_i\,\partial x_j} = 0. \tag{2}$$

Here, u_i are the particle displacements measured along the three Cartesian axes x_i ($x_1=x$, $x_2=y$, and $x_3=z$). The elastic stiffness tensor c_{ijkl} has six independent elastic constants c_{11}, c_{12}, c_{13}, c_{33}, c_{44}, and c_{66} (in Voigt two-index notation) for the hexagonal crystals (AlN and GaN). For the trigonal crystal (Al_2O_3), c_{14} is additionally an independent elastic constant. Note that the nonzero value of c_{14} gives rise to the polarization mixture of the SAWs propagating on a C-plane.[11] We have taken into account the piezoelectric coupling, and so the anisotropic Laplace's equation for the potential Φ is inter-coupled to the elastic wave equations for u_i by the piezoelectric tensor e_{ijk}. The density of the medium is ρ and ε_{ij} is the dielectric permittivity.

In Fig. 2, we compare the dispersions of the fundamental SAW mode when the layer thicknesses are systematically varied. The direction of the SAW propagation is set to be along high-symmetry directions, i.e., along the [11$\bar{2}$0] direction of Al_2O_3 in Fig. 2(a) and along the [1$\bar{1}$00] direction of Al_2O_3 in Fig. 2(b). The Al_2O_3 substrate generally mixes the sagittal and transversal polarizations of SAWs. The mixing is, however, absent if the SAW propagation is exactly along the [1$\bar{1}$00] direction of Al_2O_3.

The dispersion is similar for the two propagation directions. Here, the ratio of the layer thicknesses d_{AlN}/d_{GaN} is

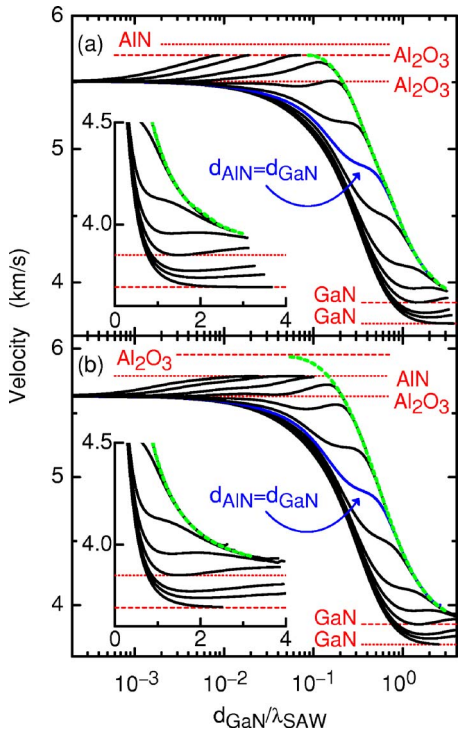

FIG. 2. (Color online) Dispersion of the fundamental SAW mode having a wavelength λ_{SAW} in AlN/GaN/Al_2O_3(0001) structures. The direction of the SAW propagation is along the (a) [11$\bar{2}$0] and (b) [1$\bar{1}$00] directions of Al_2O_3. The ratio of the thicknesses of the AlN and GaN layers d_{AlN}/d_{GaN} is 100, 50, 20, 10, 5, 2, 1, 0.5, 0.2, 0.1, 0.05, 0.02, 0.01, and 0 for the solid curves from top to bottom. The horizontal dotted and dashed lines indicate the velocities of, respectively, the SAW and the bulk transverse wave having the polarization normal to the surface in AlN, GaN, and Al_2O_3. The dashed curve is the dispersion of the interface mode, for which the AlN layer is assumed to be semi-infinitely thick. The details in the short-wavelength regime are shown in the insets.

varied from 100 to 0 for the curves from top to bottom in each panel. The bottom curve thus corresponds to a GaN/Al_2O_3 structure, for which the SAW velocity v_{SAW} decreases monotonically from that in Al_2O_3 to that in GaN with decreasing λ_{SAW}. When the GaN/Al_2O_3 structure is capped by an AlN layer, i.e., $d_{AlN}/d_{GaN}>0$, the SAW dispersion exhibits a transition from the aforementioned dispersion in the GaN/Al_2O_3 structure to the dispersion indicated by the dashed curve. The transition takes place at larger λ_{SAW} for larger d_{AlN}/d_{GaN}. The dashed curve is the dispersion of the fundamental interface mode, which has been calculated by assuming that a GaN layer is sandwiched by semi-infinite AlN and Al_2O_3, i.e., $d_{AlN}\to\infty$.

For a nonzero value of d_{AlN}, v_{SAW} in the limit of $\lambda_{SAW}\to 0$ is given by the velocity v_{T1} of the bulk transverse wave having polarization normal to the surface in GaN rather than v_{SAW} in AlN. Ordinarily, v_{SAW} in a three-component system is given by that in the substrate in the limit of $\lambda_{SAW}\to\infty$ and by that in the top layer in the limit of $\lambda_{SAW}\to 0$. The middle layer inserted between the substrate and the top layer modifies v_{SAW} in the medium wavelength regime. The SAW dispersion often develops, as a consequence, a peak or dip in this regime if the sound propagation in the middle layer is faster or slower than that in the rest of the system, respectively. The unusual saturation velocity for $\lambda_{SAW}\to 0$ in the

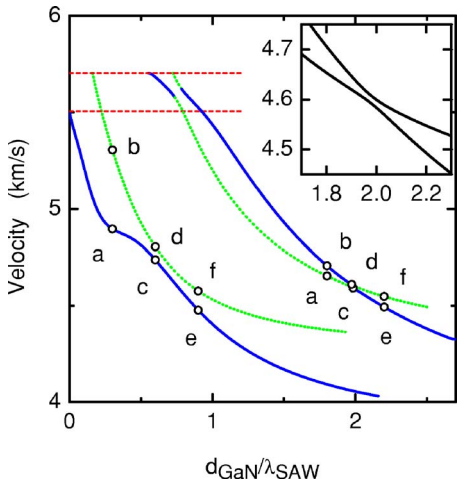

FIG. 3. (Color online) Dispersion of the lowest four modes having a wavelength of λ_{SAW} in an AlN/GaN/Al_2O_3(0001) structure. The thickness of the AlN layer is identical to that of the GaN layer d_{GaN}. The propagation direction is along $Al_2O_3[11\bar{2}0]$. The solid and dotted curves indicate the regions in which the polarization is predominantly sagittal (Rayleigh-type) and transversal (Love-type), respectively. The top and bottom horizontal dashed lines indicate the bulk transverse velocity having the polarization normal to the surface and the SAW velocity in Al_2O_3, respectively. For the two sets of points marked "a"–"f," the particle displacements are plotted in Figs. 4 and 5. The anticrossing around $d_{GaN}/\lambda_{SAW}=2$ is shown with expanded scales in the inset.

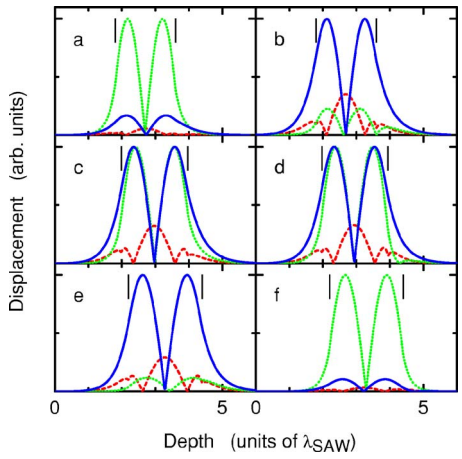

FIG. 4. (Color online) Depth profile of the displacement of particles of the medium at the points marked "a"–"f" of the third and fourth modes around $d_{GaN}/\lambda_{SAW}=2$ in Fig. 3. The dashed, dotted, and solid curves correspond to the longitudinal displacement u_1 and transversal displacements u_2 and u_3 in the in-plane and depth directions, respectively. The bars indicate the location of the heterointerfaces.

AlN/GaN/Al_2O_3 system originates from the fact that confining the particle displacements of the SAWs in the low-velocity buried GaN layer is energetically favorable to the conventional localization of the displacements at the immediate vicinity of the surface due to the extremely high velocity in the top AlN layer.[9,10] This SAW relocation from the top AlN layer to the buried GaN layer, which corresponds to the marked transition to the interface mode in Fig. 2, occurs in the short-wavelength regime when the SAWs can fit into the "acoustic well." This condition is roughly given by $\lambda_{SAW} < d_{GaN}$, but is clearly influenced by d_{AlN}, as one finds in Fig. 2.

The velocity of the interface mode is given by v_{T1} in Al_2O_3 in the limit of the long wavelength. For the SAW propagation along the $[11\bar{2}0]$ direction of Al_2O_3(0001), v_{SAW} in AlN is larger than v_{T1} in Al_2O_3. In contrast, one finds that v_{T1} in Al_2O_3 is larger than v_{SAW} in AlN when the propagation is along the $[1\bar{1}00]$ direction of Al_2O_3(0001). Reflecting this velocity relationship, the upper bound of the velocity of the fundamental mode is given by v_{T1} in Al_2O_3 in Fig. 2(a) but by v_{SAW} in AlN in Fig. 2(b).

In Fig. 3, we show the dispersion of the bottom four modes for $d_{AlN}=d_{GaN}$ when the propagation is along the $[11\bar{2}0]$ direction of Al_2O_3. We have found that the polarization is interchanged for the third and fourth modes while λ_{SAW} is varied. The solid and dotted curves indicate the regions in which the dominant polarization is sagittal and transversal, respectively. The polarization alteration suggests that the dispersion curves of the first excited Rayleigh-type mode and the second Love-type mode cross each other at $d_{GaN}/\lambda_{SAW}\approx 0.75$ and 2 if the modes were decoupled.[12] Due to the polarization mixing caused by the Al_2O_3 substrate, the mode degeneracies result in anticrossings of the dispersion curves. (The anticrossing at $d_{GaN}/\lambda_{SAW}\approx 2$ is shown with expanded scales in the inset of Fig. 3.) We show in Fig. 4 the depth profile of the particle displacements at the points marked "a"–"f" around $d_{GaN}/\lambda_{SAW}=2$ for the third and fourth modes in Fig. 3. The sagittal and transversal displacements are indeed comparable in amplitude at the anticrossing point marked "c" and "d." Similar behavior is found also for the anticrossing at $d_{GaN}/\lambda_{SAW}\approx 0.75$ (not shown).

The dominant polarization remains unchanged for the bottom two modes. However, the polarization mixing is found to be enhanced when the two dispersion curves come close to each other. Figure 5 shows the depth profile of the particle displacements at the points marked "a"–"f" around $d_{GaN}/\lambda_{SAW}=0.5$ of the bottom two modes in Fig. 3. The polarization mixing is maximized around the points marked "c" and "d." Such an enhancement of the polarization mixing is in accordance with the experimental observation[11] of the

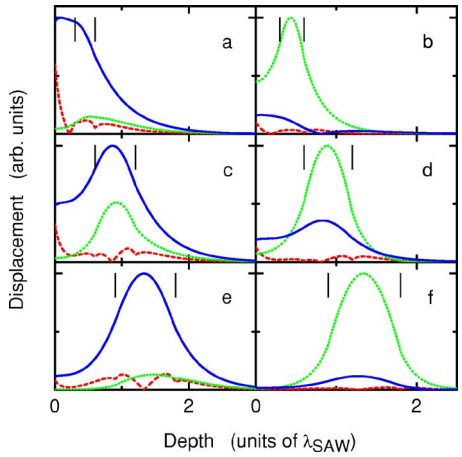

FIG. 5. (Color online) Depth profile of the displacement of particles of the medium at the points marked "a"–"f" of the lowest two modes around $d_{GaN}/\lambda_{SAW}=0.5$ in Fig. 3. The dashed, dotted, and solid curves correspond to the longitudinal displacement u_1 and transversal displacements u_2 and u_3 in the in-plane and depth directions, respectively. The bars indicate the location of the heterointerfaces.

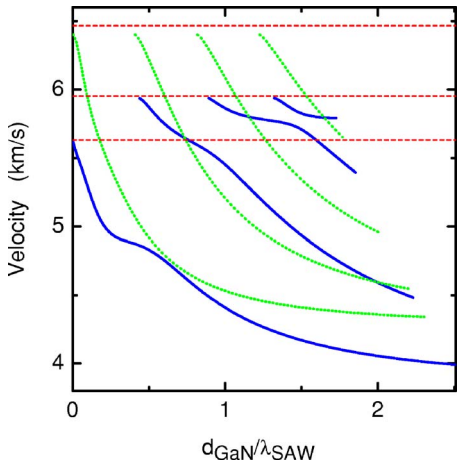

FIG. 6. (Color online) Dispersion of the lower-lying modes having a wavelength of λ_{SAW} in an AlN/GaN/Al_2O_3(0001) structure when the propagation direction is along $Al_2O_3[1\bar{1}00]$. The solid and dotted curves correspond to the Rayleigh-like and Love-type modes, respectively. The thicknesses of the AlN and GaN layers are identical ($=d_{GaN}$). The horizontal dashed lines indicate from top to bottom the bulk transverse velocities having the polarization normal to the surface and in-plane, and SAW velocity in Al_2O_3 for $[1\bar{1}00]$ propagation, respectively.

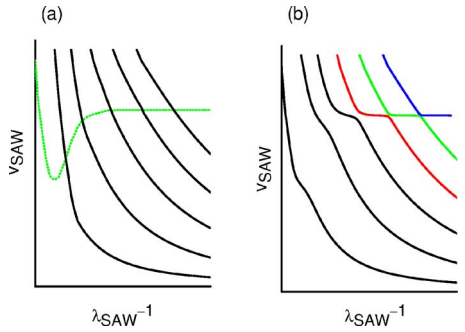

FIG. 7. (Color online) Interpretation of the dispersion in a system consisting of an AlN/GaN bilayer and a substrate in terms of mode coupling. We assume two kinds of acoustic modes whose dispersion behaves as schematically shown in (a) when they are decoupled. A coupling between the modes shown by the dotted and solid curves in (a) gives rise to anticrossings, as illustrated in (b).

excitation of the Love-type mode using interdigital transducers (IDTs) in the region of the mode proximity. Shear-horizontal SAWs are attractive, for instance, for biosensing applications,[13] as their damping resulting from the loading of biofluidic materials is negligible.[14] We note that the emergence of the acoustic vibration in the sagittal plane, which enables the excitation of the Love-type mode by IDTs, also leads to a damping when the SAW propagation path is loaded with fluid. It is thus desirable for such applications that the SAW condition be shifted away from the mode proximity region after the launch of the Love-type mode from IDTs, for instance, by adiabatically varying the layer thickness.

The SAW dispersion when the propagation is along the $[1\bar{1}00]$ direction of Al_2O_3 is shown in Fig. 6. We emphasize that the polarization mixing is absent for this propagation direction. The modes, therefore, are unambiguously identified as Rayleigh-type and Love-type modes, as indicated by the solid and dotted curves, respectively. Similar to the resemblance between the dispersions plotted in Figs. 2(a) and 2(b), the dispersion of the higher-lying modes is also qualitatively the same between the $[11\bar{2}0]$ and $[1\bar{1}00]$ propagations. One can clearly see that the polarization mixing is indeed responsible for the presence and absence of the anticrossing for the propagation directions of $[11\bar{2}0]$ and $[1\bar{1}00]$, respectively. It is also apparent that the anticrossing-like shape in the dispersion curves of the bottom two modes is actually not an anticrossing as the two curves do not cross with each other in Fig. 6 despite the absence of the coupling. Although the polarization does not mix at all at the crossing of the Rayleigh-type and Love-type modes, the Love-type mode was observed to be excited using IDTs[15] even when the propagation was along the $[1\bar{1}00]$ direction of Al_2O_3.[11] We speculate that the excitation resulted from a misalignment of the IDTs from the $[1\bar{1}00]$ direction or an incidental mixing of the polarization caused by imperfections in the experimental crystals.

Due to the transversal polarization, the velocity of the Love-type modes at the threshold is given in Fig. 6 approximately by the bulk transverse velocity in Al_2O_3 having the polarization in the surface plane. The threshold velocity of the Love-type modes is, in fact, slightly smaller than the velocity of the transversal bulk mode, as Love modes exist in layered structures only if the velocity of the transversal bulk wave in the layer is smaller than that of the equivalent modes in the substrate. (Pure transversally polarized surface modes in homogeneous systems, e.g., the Bleustein-Gulyaev-Shimizu wave, exist under specific conditions that are not fulfilled in our system.) For the higher-order Rayleigh-type modes, v_{T1} in Al_2O_3 is the threshold velocity. In contrast, the threshold velocity for the nonfundamental (non-leaky) modes in Fig. 3 is given universally by v_{T1} in Al_2O_3 due to the polarization mixing.

In Ref. 10, the dispersion of higher-order Rayleigh-type modes in an AlN/GaN/SiC system was found to develop plateaus at v_{SAW} and v_T in AlN. In passing the plateaus, the dispersion curve switched to the branch which would have belonged to the adjacent higher-order mode if it were not for the plateaus. Such slips are also recognizable for the higher-lying Rayleigh-type modes in Fig. 6. We again find the following characteristics which were revealed for the case of the SiC substrate[10] (not shown): The decay of the displacements in the depth direction resembles that of an ordinary Rayleigh mode in the plateau region at v_{SAW}. (In the plateau region at v_T for the AlN/GaN/SiC system, the finite displacement part is almost localized in the AlN layer, i.e., the decay bears a resemblance to that of the first-order Rayleigh-type mode.[10]) Away from the plateau region, the displacements contain several nodes in the depth profile in the GaN layer, in which the acoustic modes are concentrated. The number of nodes in the GaN layer differs by one in the two sides of a plateau.

The features in the dispersion of the surface modes in the AlN/GaN/Al_2O_3 system, including the mode slips, can be explained in terms of a coupling between two kinds of acoustic modes, as we propose in Fig. 7. We assume that the system sustains the two types of dispersion curves shown in

Fig. 7(a) in the absence of the coupling. The dotted line is a naively expected SAW dispersion in the $AlN/GaN/Al_2O_3$ system. Starting from v_{SAW} in Al_2O_3 in the limit of infinite λ_{SAW}, the velocity initially decreases as λ_{SAW} is shortened due to the slow sound propagation in GaN. In the limit of $\lambda_{SAW} \rightarrow 0$, the velocity saturates at v_{SAW} in AlN. The minimum in the velocity at an intermediate wavelength is a consequence that the sound propagation is slowest in the GaN layer. Similarly, the solid lines in Fig. 7(a) are the dispersion of higher-order Rayleigh-type modes in a hard-supported layered system that one would expect in a simple circumstance. Here, the velocity at the mode thresholds is given by v_{T1} in the Al_2O_3 substrate. The velocity decreases monotonically with decreasing λ_{SAW}. We have taken into account the SAW relocation effect, and so the velocity is assumed to saturate at v_{T1} in GaN in the limit of $\lambda_{SAW} \rightarrow 0$. When a coupling between these two kinds of modes is introduced, the crossing points will turn into anticrossings, as depicted in Fig. 7(b). The dispersion of the higher-lying modes is naturally expected to develop a plateau. In passing the plateau region, the characteristics of the mode change among those of the three element modes in Fig. 7(a) that constitute a single dispersion curve in Fig. 7(b). This explains the aforementioned variation in the depth profile of the particle displacements.

In conclusion, we have investigated the dispersion of SAWs in an $AlN/GaN/Al_2O_3(0001)$ system. The SAW dispersion in the short-wavelength regime is characterized by the dispersion of the fundamental mode localized in the GaN layer. The transition to the SAW confinement in the buried layer takes place at larger wavelengths when the AlN layer is thickened. While the dispersion curves are similar between the $[11\bar{2}0]$ and $[\bar{1}100]$ propagations, the polarization mixing has been found to give rise to anticrossings of Rayleigh-like and Love-like modes for the $[11\bar{2}0]$ propagation. We have demonstrated that the overall features in the SAW dispersion can be understood if we consider a coupling between two kinds of acoustic modes that primitively reflect the nature of the fundamental and guided modes.

[1] S. Strite and H. Morkoç, J. Vac. Sci. Technol. B **10**, 1237 (1992).
[2] H. Okano, N. Tanaka, Y. Takahashi, T. Tanaka, K. Shibata, and S. Nakano, Appl. Phys. Lett. **64**, 166 (1994).
[3] C. Deger, E. Born, H. Angerer, O. Ambacher, M. Stutzmann, J. Hornsteiner, E. Riha, and G. Fischerauer, Appl. Phys. Lett. **72**, 2400 (1998).
[4] Y. Takagaki, P. V. Santos, E. Wiebicke, O. Brandt, H.-P. Schönherr, and K. H. Ploog, Appl. Phys. Lett. **81**, 2538 (2002).
[5] Y. Takagaki, T. Hesjedal, O. Brandt, and K. H. Ploog, Semicond. Sci. Technol. **19**, 256 (2004).
[6] Y. Takagaki, P. V. Santos, E. Wiebicke, O. Brandt, H.-P. Schönherr, and K. H. Ploog, Phys. Rev. B **66**, 155439 (2002).
[7] C. Caliendo, Appl. Phys. Lett. **83**, 4851 (2003).
[8] G. Bu, D. Ciplys, M. Shur, L. J. Schowalter, S. Schujman, and R. Gaska, Appl. Phys. Lett. **84**, 4611 (2004).
[9] Y. Takagaki, E. Chilla, and K. H. Ploog, J. Appl. Phys. **97**, 034902 (2005).
[10] Y. Takagaki and K. H. Ploog, Semicond. Sci. Technol. **20**, 856 (2005).
[11] J. Pedrós, F. Calle, J. Grajal, R. J. Jiménez Riobóo, Y. Takagaki, K. H. Ploog, and Z. Bougrioua, Phys. Rev. B **72**, 075306 (2005).
[12] G. McHale, M. I. Newton, F. Martin, E. Gizeli, and K. A. Melzak, Appl. Phys. Lett. **79**, 3542 (2001).
[13] For a review, see "Special Issue on Acoustic Sensors" in IEEE Trans. Ultrason. Ferroelectr. Freq. Control **UFFC-34**, 122 (1987).
[14] J. Xu, J. S. Thakur, F. Zhong, H. Ying, and G. W. Auner, J. Appl. Phys. **96**, 212 (2004).
[15] Note that shear horizontal modes can be excited by IDTs on specifically-cut surfaces of some piezoelectric materials, as reviewed in M. Yamaguchi, Jpn. J. Appl. Phys., Part 1 **42**, 2909 (2003).